

Transonic Aerodynamic Computations for a Canard Configuration

Nada Agrell*

FFA, The Aeronautical Research Institute of Sweden, Bromma, Sweden
and

Lorentz Elmeland†

SAAB-SCANIA AB, Linköping, Sweden

The transonic small-perturbation (TSP) method and a linearized panel method have been used to evaluate aerodynamic derivatives for a canard configuration of low aspect ratio. The results obtained by these two methods are compared with each other at applicable Mach numbers and also with wind tunnel data covering the Mach number range to 2. For an angle-of-attack case the TSP method gives too low a lift coefficient, while the panel method gives much better agreement with tests. However, TSP shows the same trend as experiments. For an elevon deflection case, both calculation methods overpredict the aerodynamic derivatives. The experience gained in using both computational methods and comparing them with experimental results is especially important when evaluating an elastic configuration where no wind tunnel results are available. The agreement obtained for the elastic elevon deflection effectiveness by the two computation methods is very good despite the fact that the aerodynamic derivatives for the corresponding rigid configuration differ considerably.

Nomenclature

b	= span of the airplane
c	= local chord
C_L	= lift coefficient
C_l	= rolling moment coefficient
C_m	= pitching moment coefficient
C_p	= pressure coefficient
D	= deformation matrix
l	= aerodynamic load
M_∞	= freestream Mach number
q	= dynamic pressure
U_∞	= freestream velocity
x, y, z	= Cartesian coordinates
α	= angle of attack
α_e	= local mean line slope of loaded elastic wing
α_r	= local mean line slope of unloaded wing
γ	= specific heat ratio
$\Delta\alpha$	= deformation of elastic wing
δ_a	= aileron angle
δ_e	= elevon angle
δ_w	= average wing thickness ratio
ϵ	= scaling factor
η	= ratio of aerodynamic coefficients of deformed and undeformed wings
Φ	= total velocity potential
ϕ	= perturbation velocity potential

Introduction

THE linearized panel method of Ref. 1 is considered simple and inexpensive, and provides sufficiently good results in its applicable Mach number region, but, of course,

it is insufficient in the transonic range of Mach number, where other methods must be used.

The transonic small-perturbation (TSP) potential method used herein can treat a fuselage and two wing surfaces with wakes. The evaluation of steady aeroelastic effects is an option in the method. The vortex roll up and leading-edge separation are neglected. The method has been tested earlier and the results have been published in Ref. 2.

A close-coupled canard-wing configuration of low aspect ratio (Fig. 1) has been investigated using the two methods and a rigid model has been tested in the wind tunnel. These results are presented and analyzed herein.

First, a comparison between calculation and experiment is made for the rigid configuration in order to learn how the two computational methods compare with each other and with the experiments. The next step of the investigation is to use both computational methods for an elastic configuration. The interest in this case is centered around the transonic region, where the panel method is not valid and the aeroelastic effects have their extreme values.

Equations and Boundary Conditions

The basic TSP method is described in more detail in Ref. 3; only a summary will be given here.

A perturbation potential ϕ is defined in terms of the full velocity potential Φ ,

$$\Phi(x, y, z) = U_\infty [x + \epsilon \phi(x, y, z)] \quad (1)$$

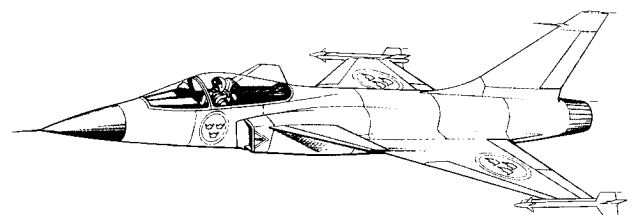


Fig. 1 View of the investigated canard-wing configuration.

Presented as Paper 84-2158 at the AIAA 2nd Applied Aerodynamics Conference, Seattle, Wash., Aug. 21-23, 1984; received Jan. 1, 1985; revision received April 12, 1985. Copyright © American Institute of Aeronautics and Astronautics, Inc., 1985. All rights reserved.

*Research Scientist, Aerodynamic Department.

†Head, Applied Aerodynamics, Aircraft Sector.

where ϵ is the scaling factor equal to $\delta_v^{3/2}/M_\infty$. The transonic small-disturbance equation is written in ϕ as follows:

$$\{(1-M_\infty^2) - [3 - (2-\gamma)M_\infty^2]M_\infty^2\epsilon\phi_x\}\phi_{xx} + \phi_{yy} + \phi_{zz} = 0 \quad (2)$$

The equation is transformed into finite difference form and solved by the successive line over-relaxation procedure introduced by Murman and Cole.⁴

At the wing and canard surfaces, no mass flux is permitted through the surface $z(x,y)$. The boundary condition⁵

$$\phi_z = \left\{ \frac{1}{\epsilon} + (1-M_\infty^2)\phi_x - \frac{1}{2}[3 - (2-\gamma)M_\infty^2]M_\infty^2\epsilon\phi_x^2 \right\} \times \frac{dz}{dx} + \phi_y \frac{dz}{dy} \quad (3)$$

is applied at their mean chord planes. For the body boundary points, the velocity vector is required to be parallel to the configuration surface. The boundary condition is given by

$$\phi_z = [(1/\epsilon) + \phi_x]f_x + \phi_y f_y \quad (4)$$

where $z=f(x,y)$ describes the body surface.

A consistent pressure coefficient⁵ has been used, namely,

$$C_p = -2\epsilon\phi_x - \epsilon^2[(1-M_\infty^2)\phi_x^2 + \phi_y^2 + \phi_z^2] + \epsilon^3[3 - (2-\gamma)M_\infty^2]M_\infty^2\phi_x^3/3$$

Across the vortex wakes there is a jump in the perturbation velocity potential ϕ . This jump is considered to be a boundary condition at the grid points bordering the wakes. The boundary conditions at the outer boundaries of the computational domain are treated somewhat differently depending on whether the freestream flow is subsonic or supersonic. Details of this treatment are given in Ref. 2.

Treatment of Steady-State Aeroelastic Effects

The wing deformation due to vertical load, l , is expressed as rotation $\Delta\alpha$ about an axis normal to the symmetry plane of the aircraft. The deformations are linear functions of the loads for small wing deflections

$$\{\Delta\alpha\} = [D] \{l\}$$

where D is the deformation matrix. D can either be evaluated from deformation measurements on a real wing, or it can be calculated by some structural method for a fictitious wing. If α_r is the slope of the wing camberline when unloaded, then

$$\{\alpha_e\} = \{\alpha_r\} + \{\Delta\alpha\}$$

An iterative procedure is used in the TSP method in order to reach an equilibrium between applied aerodynamic loading and the elastic forces arising in the deformed structure. The iterative procedure is described in more detail in Ref. 2.

Numerical Procedure

As previously mentioned, the successive line over-relaxation procedure is used to solve Eq. (2) in finite difference form. The set of difference equations containing unknowns on a vertical (to the wing plane) line is solved simultaneously. The solution procedure starts at the first upstream x station of the computational mesh and continues at subsequent x stations. The solution at each x station is obtained by line over-relaxation in an outward direction from the plane of symmetry of the configuration.

In one relaxation cycle at subsonic freestream Mach numbers, each vertical line is calculated only once. At super-

sonic freestream Mach numbers, each x plane is recalculated until a specified degree of convergence has been obtained.

When the relaxation procedure is applied to an elastic wing, the local angles of attack due to loading are evaluated as described in the previous section. The computational procedure is usually started from the solution of a rigid configuration. Thus, the changes in local angles of attack are overpredicted, and must be underrelaxed to obtain fast and sure convergence. Several flow relaxation cycles are performed for subsonic freestream Mach numbers before a re-evaluation of the deformation is made, while only one cycle is performed for supersonic freestream Mach numbers between the two successive evaluations of the deformations.

Results

The model investigated is a close-coupled canard-wing configuration of low aspect ratio, Fig. 1. For computational convenience, the fuselage of the actual configuration is approximated by a cylindrical body with a pointed nose. The canard and main wing are in different planes, with their wakes constrained to lie in these planes. On the tip of the main wing, a flat plate is used to simulate the wing tip launcher and missile.

Panel method calculations have been carried out for $0 < M_\infty < 0.9$ and $1.2 < M_\infty < 2$. The method treats either pure subsonic or pure supersonic flow and it is known that configurations within this range of aspect ratios and thicknesses at transonic speeds are beyond the scope of the method. The TSP method has been used closer to Mach number unity until calculations became limited by convergence problems and also, for comparison purposes, at Mach numbers far from unity where both methods should be valid.

The finest grid used for TSP computations was $57 \times 38 \times 35$ points. The canard was then described by 36 points

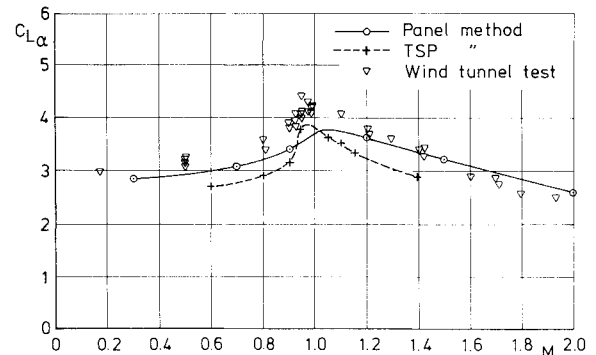


Fig. 2 Lift due to angle of attack as a function of Mach number for a rigid configuration.

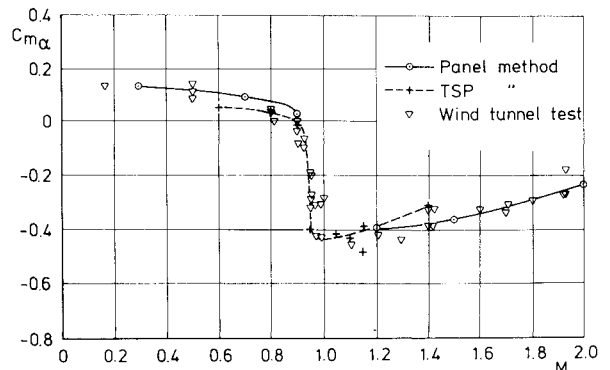


Fig. 3 Pitching moment due to angle of attack as a function of Mach number for a rigid configuration.

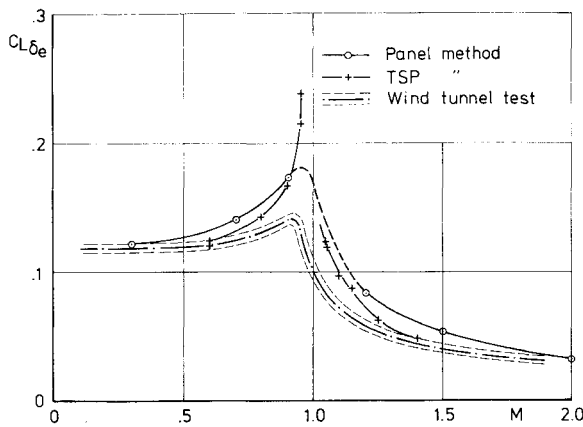


Fig. 4 Lift due to elevon deflection as a function of Mach number for a rigid configuration.

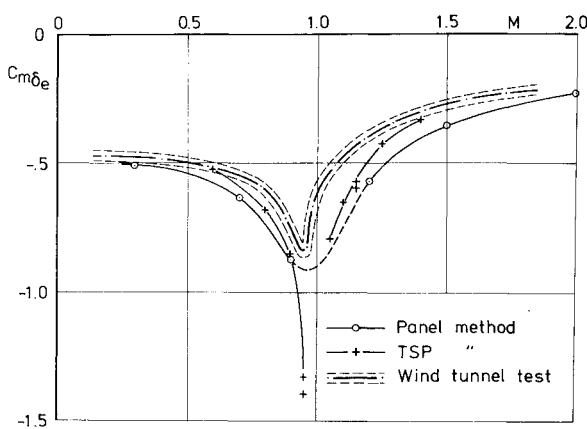


Fig. 5 Pitching moment due to elevon deflection as a function of Mach number for a rigid configuration.

and the main wing together with the flat plate at its tip by 328 points.

Figure 2 shows $C_{L\alpha}$ as a function of Mach number. Values obtained from the TSP calculations have been corrected using the panel method for an inaccurate evaluation of $C_{L\alpha}$ in the nose region of the body. The trend of $C_{L\alpha}$ with Mach number is well represented by the TSP calculation according to wind tunnel tests, while the level of $C_{L\alpha}$ is represented better by the panel method.

Figure 3 shows $C_{m\alpha}$ obtained from the TSP and panel method calculations together with the results from experiments. The agreement everywhere is very good. The TSP and panel method results complement each other very satisfactorily.

Figures 4 and 5 show the aerodynamic coefficients $C_{L\delta_e}$ and $C_{m\delta_e}$, which describe the effect of wing trailing-edge elevon deflection. Both calculation methods overpredict these coefficients greatly. The absent viscous and higher-order effects are important for these cases. The values obtained by the TSP method lie somewhere between the experimental results and the values calculated by the panel method. It can also be seen that, in the region close to $M_\infty = 1$, calculations and test results differ more for the elevon case than for the angle-of-attack case.

The computational geometry is simplified with respect to body shape and wing camber, compared to the wind tunnel model. To be able to compare pressure distributions, the difference in pressure coefficients obtained from a change in angle of attack (or elevon deflection) has been evaluated from the wind tunnel tests and the calculations. An example is shown in Fig. 6 for two span stations at $M_\infty = 1.2$.

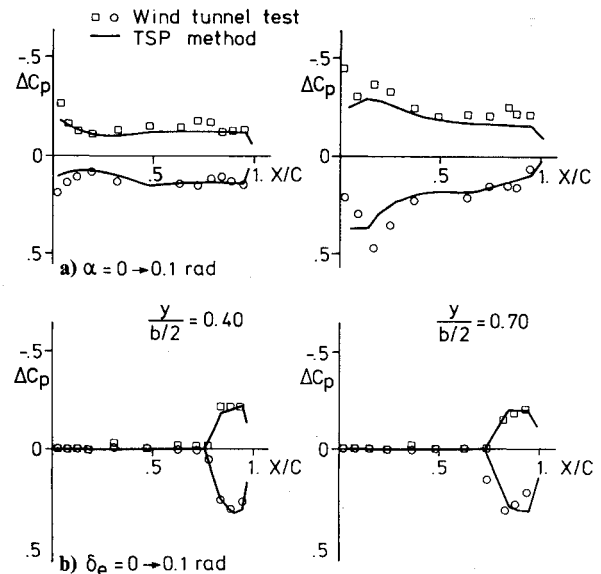


Fig. 6 Pressure distribution change for a rigid configuration at $M_\infty = 1.2$ due to an increase in a) angle of attack and b) elevon deflection.

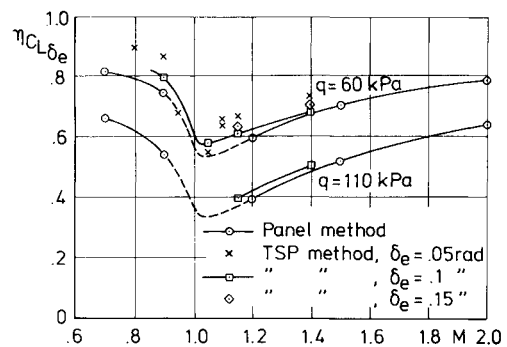


Fig. 7 Effect of aeroelasticity on lift due to elevon deflection.

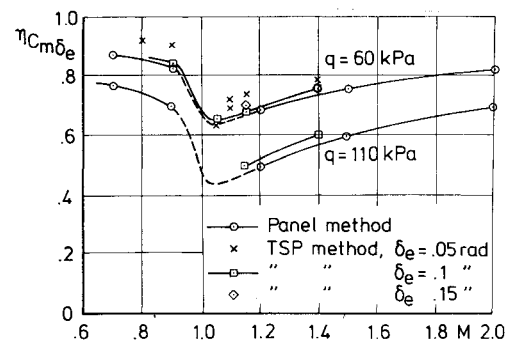


Fig. 8 Effect of aeroelasticity on elevon effectiveness.

Finally, the important effect of static aeroelasticity, as calculated by the TSP method, is examined. The effectiveness parameter is defined as a ratio of the aerodynamic derivative for the elastic configuration and the corresponding derivative for the rigid configuration

$$\eta_{C_{xy}} = \frac{(C_{xy})_{\text{elastic}}}{(C_{xy})_{\text{rigid}}}$$

where x is the lift, pitching, or rolling moment, y is the angle of attack α , or elevon deflection δ_e . The effectiveness parameters for $C_{L\delta_e}$, $C_{m\delta_e}$ and $C_{l\delta_a}$ are shown at two dynamic pressures in Figs. 7-9.

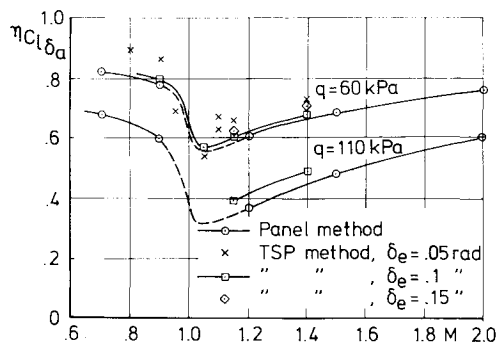


Fig. 9 Effect of aeroelasticity on aileron effectiveness.

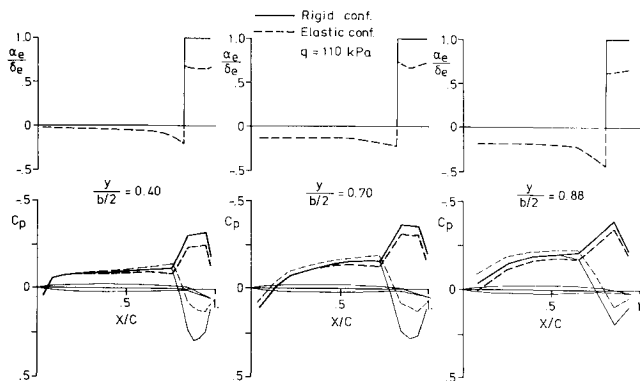


Fig. 10 Wing local slopes and surface pressures for rigid and elastic configurations at $M_\infty = 1.15$.

The TSP method cannot treat the antisymmetric aileron case. The values here have been evaluated from symmetric elevon deflections. The feasibility of this technique has been demonstrated by comparisons using the panel method. Initial calculations were made for a small elevon deflection ($\delta_e = 0.05$ rad). The results had large scatter and were very different from those obtained and expected by the panel method. When larger elevon deflection was applied, the effectiveness parameters decreased to the values computed by the panel method in the region where both methods should compare. This is surprising, however, since Figs. 2-5 show that the two methods do not agree very well for the rigid configuration. The shape of the TSP curve in the transonic regime in Figs. 7-9 did agree well with flight and wind tunnel tests for a similar configuration.⁶

Finally, Fig. 10 shows the pressure distributions and local slopes of the rigid and loaded elastic wings at three spanwise stations. First, it can be seen that the relative deflection of the elevon is reduced to around 70% for the particular dynamic pressure. Note also that the wing has been twisted

nose down and that the tendency becomes more pronounced when moving out along the span toward the wing tip. Both effects tend to decrease the elevon effectiveness for the elastic configuration over the rigid configuration.

Conclusions

The transonic small-perturbation method (TSP) and the linearized panel method have been employed to evaluate aerodynamic derivatives for a canard-wing configuration of low aspect ratio. The results were compared with wind tunnel data when such were available.

The panel method shows good agreement with experiment for angle of attack, while the TSP method gives too low a lift coefficient. In the transonic region, the computed TSP results show the same trends as experiments. Both methods overpredict the effect of elevon deflection, especially in the transonic region. Best results are obtained with the TSP.

The influence of static aeroelasticity on elevon effectiveness is predicted with good agreement by the two methods. This result was obtained in spite of the fact that corresponding calculated derivatives of the rigid configuration differ considerably.

The TSP method is an important complementary tool to the panel method, as the latter is not applicable for $0.9 < M_\infty < 1.2$. Thus, the TSP method is of special importance when determining aeroelastic effects that have extreme values in this region.

Acknowledgments

This investigation has been financed in part by the Air Material Department of the Swedish Defence Material Administration under Contract AU-1691. The computations with the panel method were carried out by Ulla Teige and the aeroelastic matrix was produced by Bertil Håden.

References

- Woodward, F. A., Tinoco, E. N., and Larsen, J. W., "Analysis and Design of Supersonic Wing-Body Configurations, Including Flow Properties in the Near-Field. Part I—Theory and Application," NASA CR-73106, 1967.
- Agrell, N. and Hedman, S. G., "Calculations of Transonic Steady State Aeroelastic Effects for a Canard Airplane," ICAS Paper 82-2.1.2, 1982.
- Schmidt, W. and Hedman, S. G., "Recent Explorations in Relaxation Methods for Three-Dimensional Transonic Potential Flow," ICAS Paper 76-27, 1976.
- Murman, E. M. and Cole, J. D., "Calculation of Plane Steady Transonic Flows," *AIAA Journal*, Vol. 9, Jan. 1971, pp. 114-121.
- Schmidt, W., "Self-Consistent Formulation of the Transonic Small-Disturbance Theory," *Recent Developments in Theoretical and Experimental Fluid Mechanics*, edited by U. Müller, K. G. Roesner, and B. Schmidt, Springer-Verlag, Berlin 1979, pp. 44-57.
- Kloos, J. and Elmeland L., "Static Aeroelastic Effects on the SAAB 37 Viggen Aircraft. A Comparison between Calculations, Wind Tunnel Tests and Flight Tests," ICAS Paper 74-55, 1974.